5-3-2017

Kinetic theory of dark solitons with tunable friction

Hilary M. Hurst
University of Maryland, hilary.hurst@sjsu.edu

Dimitry K. Efimkin
University of Texas at Austin

I. B. Spielman
University of Maryland

Victor Galitski
University of Maryland

Kinetic theory of dark solitons with tunable friction

Hilary M. Hurst,[1] Dmitry K. Efimkin,[2] I. B. Spielman,[3] and Victor Galitski[1]
[1]*Joint Quantum Institute and Condensed Matter Theory Center, Department of Physics, University of Maryland, College Park, Maryland 20742-4111, USA*
[2]*The Center for Complex Quantum Systems, The University of Texas at Austin, Austin, Texas 78712-1192, USA*
[3]*Joint Quantum Institute, National Institute of Standards and Technology and University of Maryland, Gaithersburg, Maryland 20899, USA*
(Received 1 March 2017; published 3 May 2017)

We study controllable friction in a system consisting of a dark soliton in a one-dimensional Bose-Einstein condensate coupled to a noninteracting Fermi gas. The fermions act as impurity atoms, not part of the original condensate, that scatter off of the soliton. We study semiclassical dynamics of the dark soliton, a particlelike object with negative mass, and calculate its friction coefficient. Surprisingly, it depends periodically on the ratio of interspecies (impurity-condensate) to intraspecies (condensate-condensate) interaction strengths. By tuning this ratio, one can access a regime where the friction coefficient vanishes. We develop a general theory of stochastic dynamics for negative-mass objects and find that their dynamics are drastically different from their positive-mass counterparts: they do not undergo Brownian motion. From the exact phase-space probability distribution function (i.e., in position and velocity), we find that both the trajectory and lifetime of the soliton are altered by friction, and the soliton can undergo Brownian motion only in the presence of friction and a confining potential. These results agree qualitatively with experimental observations by Aycock *et al.* [Proc. Natl. Acad. Sci. USA **114**, 2503 (2017)] in a similar system with bosonic impurity scatterers.

DOI: 10.1103/PhysRevA.95.053604

I. INTRODUCTION

Solitons are common in physical systems, from water waves to optical pulses. These particlelike excitations propagate without changing their shape; their remarkable stability is related to the integrability of the underlying nonlinear equations describing them. Advances in ultracold quantum gases have led to experiments with precise control over the manipulation and creation of solitons. Dark solitons, associated with a dip in density, and bright solitons, associated with a bump in density, have been experimentally observed [1–5]. In the near future, more complicated structures such as vector solitons and magnetic solitons could be realized in ultracold gases. Spinor condensates, Bose-Fermi mixtures, and binary condensates have all been proposed as systems for exploring exotic soliton physics [6–11]. Furthermore, solitons in quantum gases are close relatives of magnetic solitons in solid-state systems, such as domain walls and skyrmions, which have been proposed as candidates for information storage [12–16]. Theoretical understanding of how dissipation and noise affects solitons is essential for their incorporation in future technologies.

Matter-wave dark solitons in Bose-Einstein condensates (BECs) are ideal probes of both classical and quantum dynamics. Their heavy mass and localized nature allow their dynamics to be understood classically. However, they are also highly sensitive to dimensionality and background fluctuations [17]. Recent years have seen renewed theoretical interest in the effects of friction and dissipation on solitons, which can greatly affect their lifetime and stability [18–25]. Additionally, the diffusion coefficient of a soliton was recently measured experimentally for the first time [26].

In the theoretical literature, dissipation in solitonic systems has been studied by including a trap or introducing additional dimensions [18,27–29]. In higher dimensions, solitons are unstable, and experimental systems must be close to one-dimensional (1D) in order to observe them. The friction coefficient of the soliton is related to the reflection coefficient of excitations scattering off of it [18,22,24,30]. In isolated Bose gases at nonzero temperature, these scatterers would be the Bogoliubov quasiparticles of the original condensate, and their reflection coefficient can be calculated for various geometries. However, in a 1D scattering theory and without a trap the Bogoliubov excitations are reflectionless and therefore do not cause Ohmic friction [21,24]. It was recently shown that non-Ohmic friction can still occur in these systems by accounting for non-Markovian effects [21]. However, experimental systems are necessarily quasi-1D; therefore, both Ohmic friction and non-Markovian friction are present.

In this work we consider an alternative way to induce Ohmic friction in a 1D system consisting of a condensate, with a dark soliton, coupled to a noninteracting cloud of fermionic "impurity" atoms. This is similar to the setup employed in Ref. [26]. We present three main results: First, the system *with* impurities can be tuned to have zero Ohmic friction based only on the ratio of interspecies (impurity-condensate) to intraspecies (condensate-condensate) interaction strengths. Second, in contrast to objects with positive mass, for a negative-mass object such as a dark soliton there is no diffusion in a meaningful sense in free space. We show that the soliton undergoes only ballistic motion due to the fact that friction increases its speed, providing an antidamping force. Third, in the presence of Ohmic friction *and* an external potential, the dark soliton can undergo diffusion or Brownian motion, characterized by a mean-square displacement that grows linearly in time, $\langle \bar{x}^2 \rangle \propto Dt$. In this case, the diffusion coefficient is $D \propto \gamma/\omega^2$, where γ is the friction coefficient and ω is the frequency of harmonic confinement. The diffusion coefficient is *proportional* to the amount of friction in the system, in contrast to the usual case where $D \propto 1/\gamma$ [31]. Dark solitons provide an ideal experimental test bed for the mechanism of trap-induced Brownian motion.

This paper is structured as follows: In Sec. II we outline the model of a dark soliton in a quasi-1D BEC in the presence of noninteracting fermions. In Sec. III we discuss the single-particle scattering properties of the fermions in the presence of the soliton, which acts as a potential well for the fermions. Section IV is devoted to kinetic theory, where we derive two essential equations: the microscopic expression for the friction coefficient and the kinetic equation for the soliton probability distribution function (PDF), which can be calculated exactly. In Sec. V, we use the PDF to calculate the soliton's average position and variance in position. We show that Brownian motion occurs only in the presence of an external trap and calculate the diffusion coefficient. We use the PDF again in Sec. VI to define and calculate the soliton lifetime. Finally, in Sec. VII we discuss possible experimental implementations of our proposal and conclude. Technical details of the calculations are left to the appendices.

II. MODEL

We consider a quasi-1D bosonic superfluid interacting with a Fermi gas in an external potential. The proposed creation and manipulation of solitons requires a highly elongated geometry with confinement frequency $\omega_{c/i,x} \ll \omega_{c/i\perp}$, where the subscript c denotes the bosons that make up the condensate, subscript i denotes fermionic impurity atoms, and $\omega_{c/i,x}$ and $\omega_{c/i\perp}$ denote the confinement frequencies for the elongated and transverse directions, respectively.

A 1D theory is sufficient to describe the quasi-1D system provided that the transverse confinement is tight enough that transverse degrees of freedom can be eliminated, conditions which we enumerate below. Under these conditions, the system is described by the 1D Hamiltonian $\hat{H} = \hat{H}_c + \hat{H}_i + \hat{H}_{int}$,

$$\hat{H}_c = \int dx \frac{\hbar^2}{2m_c} \nabla\hat{\phi}^\dagger \nabla\hat{\phi} + U(x)\hat{\phi}^\dagger\hat{\phi} + \frac{g}{2}\hat{\phi}^\dagger\hat{\phi}^\dagger\hat{\phi}\hat{\phi}, \quad (1)$$

$$\hat{H}_i = \int dx \frac{\hbar^2}{2m_i} \nabla\hat{\psi}^\dagger \nabla\hat{\psi} + U(x)\hat{\psi}^\dagger\hat{\psi}, \quad (2)$$

$$\hat{H}_{int} = \int dx g' \hat{\psi}^\dagger\hat{\phi}^\dagger\hat{\phi}\hat{\psi}, \quad (3)$$

where $U(x)$ is an external potential, $\hbar$ is Planck's constant, and m_c and m_i denote the masses of the condensate and impurity atoms, respectively. The field operators are denoted $\hat{\phi}$ for bosons and $\hat{\psi}$ for fermions. By integrating over transverse degrees of freedom, the 1D interaction strengths are given by the well-known expressions $g = 2\hbar\omega_{c\perp}a_{cc}$ and $g' = 2\hbar\sqrt{\omega_{c\perp}\omega_{i\perp}}a_{ci}$, where a_{cc} and a_{ci} denote the three-dimensional intraspecies (boson-boson) and interspecies (boson-fermion) scattering lengths [32,33].

At very low temperatures the bosons undergo Bose-Einstein condensation. Provided that the bosons are weakly interacting ($gn_c \ll 1$, where n_c is the density), we can make the mean-field approximation $\langle\hat{\phi}\rangle \to \phi_0$. The field ϕ_0 denotes the macroscopic wave function of the condensate, which obeys the Gross-Pitaevskii equation (GPE)

$$i\hbar\frac{\partial\phi_0}{\partial t} = -\frac{\hbar^2}{2m_c}\frac{\partial^2\phi_0}{\partial x^2} + U(x)\phi_0 + g|\phi_0|^2\phi_0 + g'n_i\phi_0, \quad (4)$$

where $n_i = \langle\hat{\psi}^\dagger\hat{\psi}\rangle$ is the impurity density.

The condensate profile then appears as an external potential $V(x) = |\phi_0(x)|^2$ for the impurity atoms, which we treat using a single-particle model. The single-particle wave function of the fermions, denoted ψ, obeys the Schrödinger equation

$$i\hbar\frac{\partial\psi}{\partial t} = -\frac{\hbar^2}{2m_i}\frac{\partial^2\psi}{\partial x^2} + U(x)\psi + g'|\phi_0|^2\psi. \quad (5)$$

Hamiltonian equations (1)–(3) apply to both bosonic and fermionic impurities; in this work we consider the latter. Such Bose-Fermi mixtures have been realized experimentally and have been shown to be stable in quasi-1D [33–39]. In order for our 1D theory to be applicable, the system must be in the quasi-1D regime. This corresponds to the conditions $\mu_c \ll \hbar\omega_{c\perp}$ for the condensate and $\mu_i \ll \hbar\omega_{i\perp}$ for the impurity atoms, where $\mu_{c,i}$ are the chemical potential of the condensate and impurities, respectively.

In the microscopic theory, the harmonic potential $U(x)$ is assumed to be sufficiently shallow such that $l_t \gg \xi$, where $l_t = \sqrt{\hbar/m_c\omega_{c,x}}$ is the effective length scale of the trap and ξ is the healing length of the condensate. Therefore, the trap only weakly affects the solutions to Eqs. (4) and (5), and we set $U(x) = 0$ in the following. The background (Thomas-Fermi) confining potential provided by the BEC in a trap will, however, be important when we consider the semiclassical dynamics of the soliton in later sections.

Under the assumption $U(x) = 0$, Eq. (4) is known to have dark-soliton solutions of the form $\phi_0(x,t) = \tilde{\phi}_0(x - v_s t)e^{-i\mu_c t/\hbar}$, with

$$\tilde{\phi}_0(x - v_s t) = \sqrt{n_c}\left[i\frac{v_s}{c} + \gamma_s \tanh\left(\gamma_s\frac{x - v_s t}{\sqrt{2}\xi}\right)\right], \quad (6)$$

where v_s denotes the soliton velocity, n_c is the density of the condensate as $x \to \pm\infty$, $c = \sqrt{\mu_c/m_c}$ is the speed of sound in the condensate with chemical potential $\mu_c = gn_c$, $\gamma_s^2 = 1 - v_s^2/c^2$, and $\xi = \hbar/\sqrt{2}m_c c$ is the condensate healing length. We have also neglected the last term in Eq. (4), $\propto g'n_i$, because at very low densities the impurity atoms do not impede soliton creation and it is safe to assume the typical dark-soliton profile for the condensate wave function [26].

We see from Eqs. 5 and (6) that the dark soliton creates a potential well for the impurity atoms. First, we analyze the single-particle scattering properties of the impurities due to the soliton well. In our further analysis we treat the soliton as a classical particle interacting with a bath of fermionic quantum scatterers, similar to the problem of a heavy particle moving through a gas of much lighter particles [40].

III. IMPURITY SCATTERING

We can rewrite Eq. (5) in the frame comoving with the soliton by making the variable transformation $z = \gamma_s(x - v_s t)/\sqrt{2}\xi$, $\psi(x,t) = e^{-iEt/\hbar}e^{ik_s z}\psi(z)$, where $k_s = m_i v_s/\hbar$. This gives the following time-independent Schrödinger equation for impurity atoms:

$$\frac{\partial^2\psi(z)}{\partial z^2} + \left[\frac{\lambda(\lambda - 1)}{\cosh^2 z} + k^2\right]\psi(z) = 0, \quad (7)$$

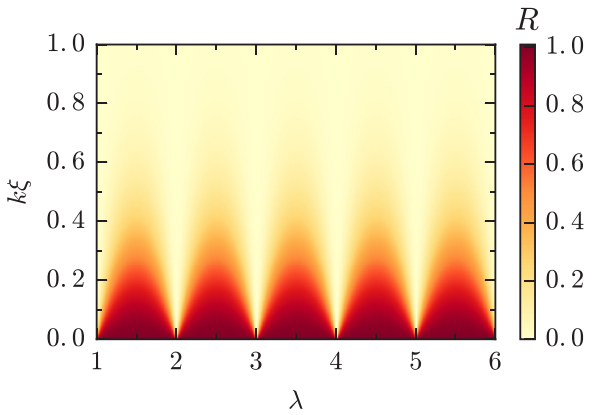

FIG. 1. The reflection coefficient $R(k,\lambda)$ as a function of λ, where $\lambda(\lambda-1)=2m_i g'/m_c g$. $R(k,\lambda)$ is strongly peaked at $k\approx 0$ and is periodic as a function of λ. When λ is an integer, $R(k,\lambda)$ is exactly zero.

where

$$\lambda(\lambda-1)=\frac{2m_i g'}{m_c g},\ k^2=\frac{4m_i\xi^2}{\hbar^2\gamma_s^2}\left(E+\frac{m_i v_s^2}{2}-g' n_c\right). \quad (8)$$

The potential in Eq. (7) is known as the Pöschl-Teller potential, whose solutions are known in closed form and which has been widely studied in the context of supersymmetric quantum mechanics [40–46]. The reflection coefficient of scattering states is

$$R(k,\lambda)=\frac{1-\cos(2\pi\lambda)}{\cosh(2\pi k)-\cos(2\pi\lambda)}. \quad (9)$$

$R(k,\lambda)$ vs λ is shown in Fig. 1. Furthermore, $R(k,\lambda)=0$ when λ takes integer values; thus, the soliton can become reflectionless to the impurities. The soliton potential well can also have bound states. The total number of bound states is the largest positive integer $j<\lambda-1$. One or two fermionic impurities may occupy each bound state in the soliton core, and these bound particles affect the phase shift of scattered impurities. The effect of bound states and scattering-state phase shifts are taken into account when we calculate the chemical potential of the fermions in Appendix A.

IV. KINETIC THEORY OF DARK SOLITONS

The energy of the soliton texture in Eq. (6) is calculated by subtracting the uniform background, and it is given by

$$E(v_s)=\frac{4\hbar n_c c}{3}\left(1-\frac{v_s^2}{c^2}\right)^{3/2}\approx\frac{4\hbar n_c c}{3}-\frac{M v_s^2}{2}. \quad (10)$$

Here we expanded $E(v_s)$ under the condition $v_s\ll c$. The soliton is effectively a particle with negative mass of magnitude $M=4\hbar n_c/c=4\sqrt{2}n_c\xi m_c$. The soliton is heavy compared to a single atom, $m_c\ll M$, with width ξ/γ_s. The heavy mass and localized nature of the dark soliton justify the following classical treatment of its dynamics [47].

We note here that M is often called the "inertial mass," whereas one can also define the "gravitational mass" M_g of a soliton, which is also negative. Gravitational mass is the missing mass of the atoms in the soliton core, given by integrating over the soliton density with the uniform background subtracted, $-M_g=m_c\int dx(n_s-n_c)$, where $n_s(x,t)=|\tilde{\phi}_0(x-v_s t)|^2$ from Eq. (6). For a stationary soliton, $M_g=2\sqrt{2}n_c\xi m_c$ and $M=2M_g$. In the case of harmonic confinement the soliton has gravitational potential energy $U(x_s)=-M_g\omega_{c,x}^2 x_s^2/2$. This distinction is important for the soliton's classical equation of motion, given by $-M\ddot{x}=M_g\omega_{c,x}^2 x$. Dark solitons are quite stable in a harmonic trap and oscillate as a classical particle would, with effective frequency $\omega=\omega_{c,x}/\sqrt{2}$ [47–49].

In order to describe the diffusive behavior of solitons, we need to understand how a soliton will deviate from the average trajectory computed for many solitons. Soliton dynamics can be most readily examined by understanding their PDF $f(t,x_s(t),v_s(t))$. The soliton PDF obeys the kinetic equation

$$\frac{\partial f}{\partial t}+v_s\frac{\partial f}{\partial x_s}+\dot{v}_s\frac{\partial f}{\partial v_s}=\mathcal{I}[f], \quad (11)$$

where the collision integral $\mathcal{I}[f]$ accounts for scattering of fermionic impurities off of the soliton. As the soliton is much heavier than the fermions, $M\gg m_i$, the transferred momentum to and from the soliton due to collisions is small. This assumption results in a collision integral of Fokker-Plank form,

$$\mathcal{I}[f]=\frac{\partial}{\partial v_s}\left(-A_{v_s}f+\frac{\partial}{\partial v_s}\left[B_{v_s}f\right]\right), \quad (12)$$

which we derive in Appendix B. The transport coefficients A_{v_s} and B_{v_s} account for drift and diffusion of the distribution and are given by

$$A_{v_s}=-\frac{2\hbar}{M}\sum_k kR_{k,\lambda}\left|\frac{\partial\epsilon_k}{\hbar\partial k}\right|n_F(\epsilon_{k+k_s})\left[1-n_F\left(\epsilon_{-k+k_s}\right)\right], \quad (13)$$

$$B_{v_s}=\frac{2\hbar^2}{M^2}\sum_k k^2R_{k,\lambda}\left|\frac{\partial\epsilon_k}{\hbar\partial k}\right|n_F(\epsilon_{k+k_s})\left[1-n_F\left(\epsilon_{-k+k_s}\right)\right], \quad (14)$$

where $n_F(\epsilon_k)$ is the Fermi-Dirac distribution for the impurity atoms, which is shifted by k_s because we calculated the reflection coefficient $R(k,\lambda)$ in the frame comoving with the soliton. The impurities have the usual dispersion relation $\epsilon_k=\hbar^2k^2/2m_i$, and the last term, $[1-n_F(\epsilon_{-k})]$, accounts for Pauli-blocking effects on impurity scattering.

To the lowest order in k_s, we expand $n_F(\epsilon_{k+k_s})$ to find $A_{v_s}=\gamma v_s/M$ and $B_{v_s}=\gamma k_B T/M^2$, where γ is given by

$$\gamma=\frac{2\hbar^2}{k_B T}\sum_k k^2R_{k,\lambda}\left|\frac{\partial\epsilon_k}{\hbar\partial k}\right|n_F(\epsilon_k)[1-n_F(\epsilon_{-k})]. \quad (15)$$

This exact expression shows that A_{v_s} and B_{v_s} are not independent but intrinsically connected via the relation $A_{v_s}=Mv_sB_{v_s}/k_BT$. This guarantees that the collision integral vanishes when $f(v_s)$ is given by the classical Maxwell-Boltzmann distribution. For a positive-mass object this corresponds to thermal equilibrium; however, for negative-mass particles the situation is more complicated.

The crucial difference between Eq. (12) and the typical collision integral for a positive-mass object is that the drift term $A_{v_s}\propto v_s$ is *negative*, indicating that over time the distribution

drifts from lower to higher velocities. Thus, Eq. (11) does not have a stationary solution. We show below that this leads to the absence of diffusion in free space, where diffusion is formally defined as variance in position that grows linearly in time, $\langle \bar{x}^2 \rangle \propto t$. The apparent unbound runaway of the distribution function is a result of the expansion of the energy in Eq. (10) for $v_s \ll c$, as discussed in further detail in Appendix C. If we consider the full energy spectrum, then the system does reach equilibrium, where the dark soliton accelerates to the speed of sound and disappears. However, to describe the initial soliton trajectory we choose to work in the regime $v_s \ll c$, where the collision integral takes the simple form given by Eq. (12).

We note that in the case of bosonic impurities, instead of a Pauli-blocking factor, there is a Bose enhancement factor, $[1 + n_B(\epsilon_{-k})]$, where n_B is the Bose-Einstein distribution. This factor has been overlooked previously [18,24], but it strongly influences the magnitude of the friction coefficient for a degenerate gas of impurities [26]. Moreover, the factor is crucial for satisfying the fundamental relation $A_{v_s} = M v_s B_{v_s}/k_B T$, which is dictated only by equilibrium properties and is not sensitive to the nature of the impurities [40].

Finally, combining Eqs. (11) and (12), we find the following Kramer's-type equation for the soliton distribution function:

$$\frac{\partial f}{\partial t} + v_s \frac{\partial f}{\partial x_s} = \frac{\partial}{\partial v_s}\left(-\Gamma v_s f - \frac{\partial_{x_s} U}{M} f + \Gamma v_{th}^2 \frac{\partial f}{\partial v_s}\right), \quad (16)$$

where $\Gamma = \gamma/M$ and $v_{th}^2 = k_B T/M$. This equation is analytically solvable in the case of harmonic confinement, $U(x_s) = -M_g \omega_{c,x}^2 x_s^2/2$. We present the full solution for the distribution function $f(t, x_s, v_s)$ in Appendix C.

The Langevin equation of motion for a single soliton can be inferred from Eq. (16), and it is given by

$$-M\ddot{x}_s = -\gamma \dot{x}_s + M\omega^2 x_s + f_s(t), \quad (17)$$

where $\omega = \omega_{c,x}/\sqrt{2}$. The stochastic Langevin force is characterized by white-noise correlations with $\langle f_s(t) \rangle = 0$ and $\langle f_s(t') f_s(t) \rangle = 2\gamma k_B T \delta(t - t')$. From this equation we see that γ plays the role of the friction coefficient.

At fixed impurity number, γ depends on three parameters: the temperature T, the parameter λ, and the chemical potential μ, which is itself a function of λ and T. Figure 2 shows γ as a function of λ for four different temperatures; γ grows over many orders of magnitude as λ is tuned from integer to half-integer values. The integral over k in Eq. (15) is strongly peaked around $k = 0$. Therefore, approximating $n_F(\epsilon_{k=0})[1 - n_F(\epsilon_{k=0})] \approx e^{-\beta \mu_i}$ and integrating over k, one finds the following expression for the friction coefficient:

$$\gamma \approx \frac{3\hbar^3 e^{-\mu_i/k_B T}}{2\pi^5 m_i k_B T \xi^4} \sin^2(\pi\lambda). \quad (18)$$

Recalling that $\lambda(\lambda - 1) = 2m_i g'/m_c g$, we see clearly that the system can be tuned to the frictionless limit where $\gamma = 0$ without changing the number of impurities. Furthermore, friction provides an antidamping force to the soliton, while the background harmonic potential provides a confining force. The interplay of friction and confinement leads to the emergence of Brownian motion in the system.

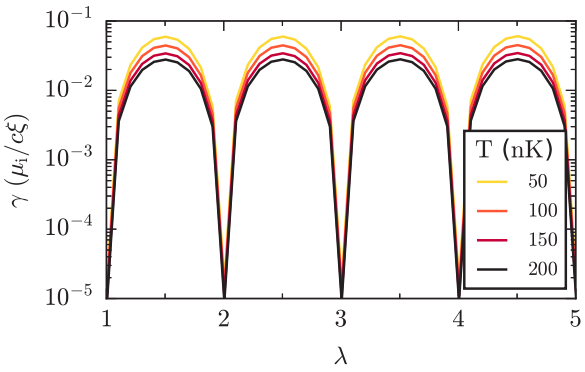

FIG. 2. The soliton friction coefficient γ is periodic as a function of λ, where $\lambda(\lambda - 1) = 2m_i g'/m_c g$. Friction vanishes for integer λ, indicating that the soliton is reflectionless to scatterers. A system with tunable interactions enables tuning γ without changing the number of scatterers. γ is calculated in units of $\mu_i/c\xi$, where μ_i is the chemical potential of impurities, c is the speed of sound in the condensate, and ξ is the condensate healing length. For impurities of ^{173}Yb as we have calculated here, γ decreases with increasing temperature. Increasingly dark lines indicate higher temperatures.

V. DARK-SOLITON TRAJECTORY

From the solution $f(t, x_s, v_s)$ of Eq. (16), we can calculate exact expectation values for the soliton position and velocity. In experiments, it is generally easier to measure soliton position, which we focus on in the following. The average soliton trajectory is given by

$$\bar{x}_s(t, \omega) = \frac{v_i e^{\Gamma t/2}}{\bar{\omega}} \sin(\bar{\omega} t), \quad (19)$$

where $\bar{\omega} = \sqrt{\omega^2 - \Gamma^2/4}$ and v_i is the initial velocity of the soliton. The variance in soliton position D_x is given by

$$D_x(t, \omega) = \frac{v_{th}^2 (e^{\Gamma t} - 1)}{\bar{\omega}^2} + \frac{v_i^2 e^{\Gamma t}}{\bar{\omega}^2} \sin^2(\bar{\omega} t) + \frac{v_{th}^2 \Gamma^2 e^{\Gamma t}}{4\omega^2 \bar{\omega}^2}\left[1 - \cos(2\bar{\omega} t) - \frac{2\bar{\omega}}{\Gamma} \sin(2\bar{\omega} t)\right]. \quad (20)$$

The problem has an intrinsic time scale given by $\Gamma^{-1} = M/\gamma$. For $\Gamma t \gtrsim 1$, the soliton's position grows exponentially, indicative of the soliton rapidly reaching the speed of sound and disappearing. We examine Eqs. (19) and (20) in the short-time limit $\Gamma t \ll 1$. The trap frequency ω also considerably affects the soliton dynamics. In the limit $\Gamma \ll \omega$, we find that diffusive behavior emerges, where $D_x(t, \omega) \propto D_0 + D(t)t$ with a time-dependent diffusion coefficient

$$\langle D(t) \rangle \approx \frac{v_{th}^2 \Gamma}{\omega^2} + \frac{v_i^2 \Gamma}{\omega^2} \sin^2(\bar{\omega} t) - \frac{v_{th}^2 \Gamma^2}{2\omega^3} \sin(2\bar{\omega} t), \quad (21)$$

with average offset $D_0 \approx v_i^2/2\omega^2 + v_{th}^2 * \Gamma^2/4\omega^4$. However, in the opposite limit of $\omega \ll \Gamma$, the linear in t term vanishes, giving

$$D_x(t, \omega) \approx v_i^2 t^2 + v_i^2 \Gamma t^3 + \tfrac{2}{3} v_{th}^2 \Gamma t^3 \quad (22)$$

to lowest order in Γt. In the absence of the restoring force provided by background potential, the soliton undergoes

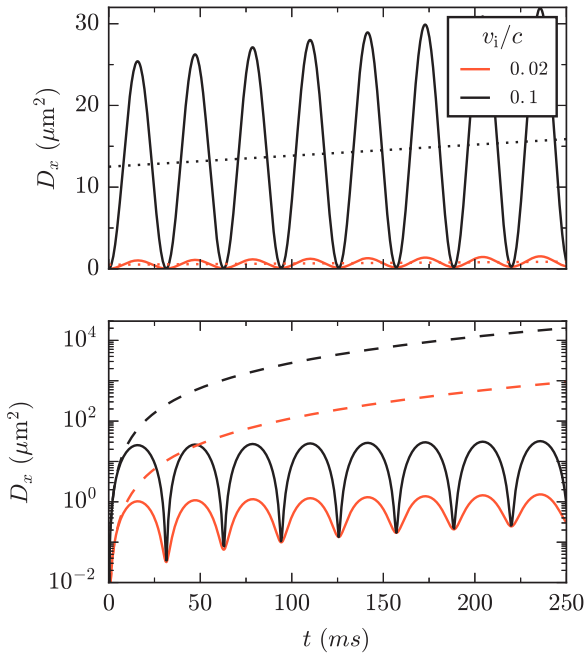

FIG. 3. Variance in soliton position $D_x(t,\omega)$ as a function of time from the exact expression (20) for $v_i/c = 0.02$ [orange (light gray) line] and $v_i/c = 0.1$ (black line) with $v_{th} \approx 0.1$ mm/s and $\Gamma^{-1} \approx 1$ s. Top: Results for a harmonic potential with $\omega = 100\Gamma$. D_x grows linearly in time with additional oscillations due to confinement. The amplitude of oscillation increases with increasing v_i. Dotted lines show the average value using the linear approximation in Eq. (21). Bottom: Comparison with $D_x(t,\omega)$ in the limit $\omega \ll \Gamma$ (dashed lines). In the absence of harmonic confinement, D_x initially grows like t^3 for $\Gamma t \ll 1$, then grows exponentially. There is no diffusive regime.

ballistic transport $\propto t^3$, followed by the exponential growth of D_x. The exact expression for $D_x(t,\omega)$ is shown in Fig. 3. The mechanism of diffusion for dark solitons is thus inherently different than Brownian motion for positive-mass objects. Friction forces cause the soliton to speed up; therefore, the only restoring force in the problem is due to the background confining potential, which leads to the emergence of diffusive behavior. Finally, we see that in the frictionless limit, $\Gamma \to 0$, we have $D \to 0$, and there is no diffusion. For quantitative agreement with experiment, the initial velocity of the soliton v_i also plays a crucial role [26].

VI. SOLITON LIFETIME

Integrating the distribution function $f(t,x_s,v_s)$ over the spatial coordinate x_s, we find the distribution of soliton velocities

$$f_v(t,v_s) = \frac{1}{\sqrt{4\pi g_3(t,\omega)}} \exp\left(-\frac{[v_s - \bar{v}_s(t)]^2}{4g_3(t,\omega)}\right), \tag{23}$$

parametrized by functions $g_3(t,\omega)$ and $\bar{v}_s(t)$. The function $g_3(t,\omega)$ is given by

$$g_3 = \frac{\{4\bar{\omega}^2(e^{\Gamma t}-1) + e^{\Gamma t}[\Gamma^2 + 2\Gamma\bar{\omega}\sin(2\bar{\omega}t) - \Gamma^2\cos(2\bar{\omega}t)]\}}{8\bar{\omega}^2}. \tag{24}$$

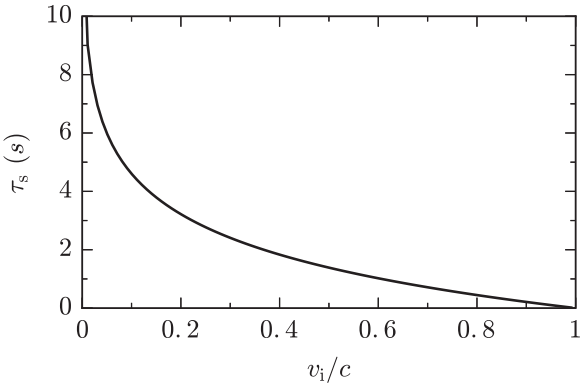

FIG. 4. Soliton lifetime as a function of initial velocity v_i, with $\omega = 100\Gamma$ and where c is the condensate speed of sound. Solitons that start at higher initial velocities have a shorter lifetime, which one would intuitively expect. Soliton lifetime is only weakly dependent on trapping frequency ω.

The average velocity is given by $\bar{v}_s(t)$, which captures oscillations in the trap as well as exponential growth of the soliton velocity,

$$\bar{v}_s(t) = \frac{v_i e^{\Gamma t/2}}{\bar{\omega}}\left[\bar{\omega}\cos(\bar{\omega}t) + \frac{\Gamma}{2}\sin(\bar{\omega}t)\right]. \tag{25}$$

Starting from the velocity distribution function in Eq. (23), we impose a perfectly absorbing boundary condition at $v_s = \pm c$, reflecting that the soliton disappears once it reaches the speed of sound. This can be done using the method of images, as discussed in detail in Appendix D. The total survival probability is defined by integrating over f_v from $-c$ to c. The final expression for survival probability is given by

$$\mathcal{P}(|v_s| < c;\tau) = \int_{-c}^{c} dv_s f_v^{\mathrm{Img}}(t,v_s), \tag{26}$$

where $f_v^{\mathrm{Img}}(t,v_s)$ is the distribution function that obeys the boundary condition $f_v^{\mathrm{Img}}(t,\pm c) = 0$ for all t. The full expression for $\mathcal{P}(|v_s| < c;\tau)$ can be found in Appendix D. From the method-of-images construction, the soliton survival probability is exactly zero when $|\bar{v}_s(t)| = c$. Using the maximum value of $\bar{v}_s(t)$ over one period, given by $\bar{v}_s^*(t) = v_i\omega e^{\Gamma t/2}/\bar{\omega}$, we define the soliton lifetime as the time τ_s where $\mathcal{P}(|v_s| < c;\tau_s) = 0$ and $|\bar{v}_s^*(\tau_s)| = c$. This gives a simple expression for the lifetime,

$$\tau_s = \frac{2M}{\gamma}\ln\left(\frac{c\bar{\omega}}{v_i\omega}\right). \tag{27}$$

The soliton lifetime from Eq. (27) is shown in Fig. 4. The lifetime decreases as initial velocity increases; however, it is only weakly dependent on the trapping frequency ω. Furthermore, soliton lifetime is simply inversely proportional to the friction coefficient γ and diverges as $\gamma \to 0$. Tuning the friction coefficient therefore should have a measurable effect in experiments, where soliton lifetime increases as γ decreases.

VII. DISCUSSION AND CONCLUSION

We calculated the friction coefficient γ and the diffusion coefficient $D(t)$ of a dark soliton in the presence of a

noninteracting Fermi gas. We have shown that the soliton acts as a potential well for the fermionic impurities, and the scattering states and reflection coefficient of the impurities can be calculated exactly.

In this section we estimate properties of a Bose-Fermi mixture of ^{174}Yb-^{173}Yb; however, the theory is general and applicable to other Bose-Fermi mixtures. We chose ^{174}Yb-^{173}Yb as a laboratory-realized example with scattering properties giving $m_i g'/m_c g \approx 1.3$ [50,51].

We consider a quasi-1D BEC of ^{174}Yb atoms with $n_c\xi \approx 100$ and speed of sound $c \approx 1$ mm/s, corresponding to a soliton mass of $M \approx 600 m_c$ and chemical potential $\mu_c \approx \hbar \times 2$ kHz. For $T = 150$ nK, the thermal velocity of the soliton is $v_{th} = \sqrt{k_B T/M} \approx 0.1$ mm/s. The chemical potential requires a radial trapping frequency of $\omega_{c\perp} \gtrsim 2\pi \times 10$ kHz for the quasi-1D criterion to be satisfied, and the shallow trapping direction should have $\omega_{c,x} \lesssim 2\pi \times 100$ Hz. We set the number of ^{173}Yb impurity atoms to $N_i = 1000$. We choose the system length $L = 250$ μm, long enough that the continuum description of the impurity scattering states is appropriate. We find the chemical potential of fermions to be on the order of $k_B T$, which requires a transverse trapping frequency $\omega_{i\perp} \gtrsim 2\pi \times 10$ kHz for the fermions to be considered one-dimensional. For lower frequencies $\omega_{i\perp}$ it is possible to obtain an accurate theory by summing over quantized transverse modes for the impurities [26].

Changing the magnitude of friction for the soliton requires tunable interactions. The most straightforward way of tuning interactions in the Yb system is by changing the overlap of the transverse wave functions of the impurities and condensate atoms. This can be done by applying optical forces to either the bosonic or fermionic species which change the overlap of the atomic clouds. The narrow linewidths in the Yb spectra are ideal for this type of selective addressing, which can be done with high precision [52]. Bose-Fermi mixtures with different atomic species allow for other ways of tuning interactions by using Feshbach resonances or magnetic field gradients [53]. For the Yb s-wave scattering lengths that have already been measured, we find $\lambda \approx 2.2$ [50]. Such a system would need to be tuned to only slightly weaker interactions such that $\lambda \approx 2$ to see a decrease in friction coefficient and corresponding measurable increase in soliton lifetime. For attractive interspecies interactions ($g' < 0$) such as in ^{87}Rb-^{40}K the soliton appears as a potential barrier rather than a well. The theory is still applicable in this case; the form of the reflection coefficient $R(k)$ is slightly different but still periodic in λ, and the physics is nominally unchanged [45].

We developed a general theory for the stochastic dynamics of negative-mass objects using a kinetic equation approach. We find that the dynamics are drastically different from their positive-mass counterparts: they do not undergo Brownian motion in free space. The proposed dark-soliton–Fermi-gas system provides an ideal experimental test bed in which to further study how friction and dissipation affect an object with negative mass.

We presented an analytical expression for the friction coefficient based on fermion scattering properties, including a term accounting for Pauli blocking, which is important to satisfy the equilibrium conditions on the transport coefficients. Using this result, we found exact expressions for the soliton position and position variance over time. We classified soliton trajectories at short times as diffusive and ballistic, and the diffusive regime can be seen only in the presence of a confining potential. The crossover time scale is given by $\Gamma^{-1} = M/\gamma$, which we find to be on the order of a second. The intrinsic frequency $\Gamma \sim 1$ Hz is very low. Thus, the time scale over which diffusive behavior occurs is on the order of seconds, and the diffusion coefficient can be directly measured [26]. Furthermore, the limit $\Gamma \ll \omega$ is justified for a reasonably shallow trapping potential which still preserves the soliton shape. Experiments with tunable interspecies interaction strength present the ability to tune the amount of friction at a fixed impurity number, providing a simple way to manipulate the lifetime and trajectory of dark solitons in a laboratory setting.

ACKNOWLEDGMENTS

This work was supported by U.S. ARO (Contract No. W911NF1310172), NSF Grant No. DMR-1613029, and the Simons Foundation (H.H. and V.G.). H.H. acknowledges additional fellowship support from the National Physical Science Consortium and NSA. Additional support was provided by the ARO's atomtronics MURI, the AFOSR's Quantum Matter MURI, NIST, and the NSF through the PFC at the JQI (I.B.S.). Part of this work was completed at the Kavli Institute for Theoretical Physics (KITP), and the authors are grateful to KITP for hospitality and for the partial support of this research from the National Science Foundation under Grant No. NSF PHY-1125915 (H.H. and V.G.).

APPENDIX A: CHEMICAL POTENTIAL OF FERMIONS

In addition to the obvious dependence on $R(k,\lambda)$, the friction coefficient γ is highly sensitive to the chemical potential of the fermionic atoms through the distribution function $n_F(\epsilon_k)$ in Eq. (15). Although the number of fermions in the system is fixed, the chemical potential is sensitive to the bound states in the soliton well, the phase shift of the scattering states, and the density of states at the Fermi level. In this appendix we present the full calculation of the chemical potential of 1D fermions in the presence of a dark-soliton potential well.

The total number of impurities is given by $N_i = N_s(\mu_i) + N_b(\mu_i) + \delta N(\mu_i)$, where N_s indicates scattering (continuum) states, N_b indicates bound states, and δN is a correction due to the phase shift of scattering states. All three quantities are a function of the chemical potential μ_i. We can define the following equation for the 1D impurity density:

$$\frac{N_i}{L} = -\sqrt{\frac{m_i k_B T}{2\pi\hbar^2}}\,\mathrm{Li}_{\frac{1}{2}}(e^{-\beta\mu_i}) + \frac{2}{L}\sum_{j=0}^{\mathrm{floor}(\lambda-1)} \frac{1}{e^{\beta(\epsilon_j-\mu_i)}+1} + \frac{1}{L}\int \frac{dk}{2\pi}\frac{1}{e^{\beta(\epsilon_k-\mu_i)}+1}\frac{\partial\delta(k,\lambda)}{\partial k}, \quad \beta = \frac{1}{k_B T}. \tag{A1}$$

The first term in Eq. (A1) comes from integrating over k for the continuum states, where $\mathrm{Li}_{1/2}(x)$ is the polylogarithm function. The continuum dispersion is $\epsilon_k \propto \hbar^2 k^2/2m_i$. The second term accounts for the bound states, which have quantized energies $\epsilon_j = -\hbar^2/2m_i\xi^2(\lambda - 1 - j)^2$ for integer $j < \lambda - 1$. The factor of 2 accounts for Pauli degeneracy. Finally, the

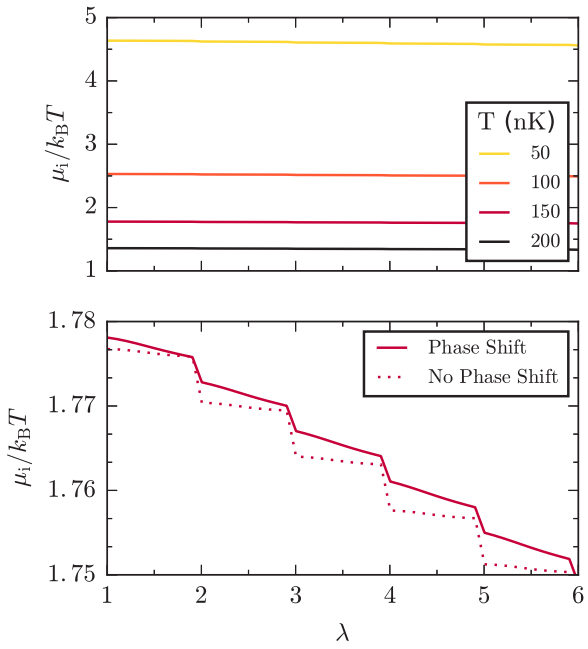

FIG. 5. Top: The chemical potential μ_i of fermionic impurities from solving Eq. (A1) numerically for $N_i = 1000$ ^{173}Yb atoms with $L = 250$ μm. μ_i decreases slightly as λ is increased and there are more bound states in the soliton well. Increasingly dark lines indicate higher temperatures. Bottom: Chemical potential for $T = 150$ nK. The steps at each integer indicate an additional bound state in the soliton well. The chemical potential including the phase shift (solid line) is increased slightly from the result without it (dotted line).

third term in Eq. (A1) is a correction due to the phase shift of the scattering states. The phase shift is given by $\delta(k,\lambda) = \mathrm{Arg}[t(k,\lambda)]$ with transmission amplitude

$$t = \frac{\Gamma(\lambda - ik)\Gamma(1-\lambda-ik)}{\Gamma(1-ik)\Gamma(-ik)} \tag{A2}$$

from the scattering matrix of Eq. (7). The correction δN is proportional to $\partial_k \delta(k,\lambda)$, which takes the form

$$\frac{\partial\delta(k,\lambda)}{\partial k} = \mathrm{Re}[\psi^0(-ik) + \psi^0(1-ik) - \psi^0(\lambda - ik) - \psi^0(1-ik-\lambda)], \tag{A3}$$

where $\psi^0(z) = \Gamma'(z)/\Gamma(z)$ is the digamma function. We solve for μ_i numerically for ^{173}Yb atoms with $N_i = 1000$ and $L = 250$ μm for temperatures $T = \{50,100,150,200\}$nK.

The results of the calculation are shown in Fig. 5. The chemical potential of the fermion atoms decreases slightly as the interaction strengths are tuned and the soliton well becomes deeper, and we find $\mu_i \approx k_B T$ for all temperatures considered. In the bottom panel of Fig. 5 we show the results with and without accounting for the phase shift term. The phase shift of the scattering states slightly increases the chemical potential. These results are used in calculating γ in Eq. (15) and Fig. 2 of the main text.

APPENDIX B: DERIVATION OF COLLISION INTEGRAL AND TRANSPORT COEFFICIENTS

The collision integral for a heavy object interacting with a gas of lighter objects can be derived in quite a general way, as has been done in many textbooks (e.g., [40,54]). The essential assumption is that the momentum transferred in each collision is small. Treating the soliton as a heavy classical object, we assume that it has some probability distribution $f(t,x_s,p)$ which depends on momentum p, time t, and position x_s. Let $P(p,q)dq$ denote the probability per unit time of a change $p \to p-q$ in the momentum of the soliton in a collision with a fermionic impurity atom, where q is the momentum transferred. The transport equation for f is then given by

$$\frac{df}{dt} = \int dq\, P(p+q,q) f(t,p+q) - P(p,q) f(t,p), \tag{B1}$$

which measures the difference between the soliton scattering into a state with momentum p and out of a state with momentum p. We assume that the transferred momentum in each collision is small, i.e., $q \ll p$, and that $P(p,q)$ is a smooth function. We then make the following expansion:

$$\begin{aligned} &P(p+q,q) f(t,p+q) \\ &\quad\approx P(p,q) f(t,p) + q\frac{\partial}{\partial p}[P(p,q) f(t,p)] \\ &\qquad + \frac{1}{2} q^2 \frac{\partial^2}{\partial p \partial p}[P(p,q) f(t,p)]. \end{aligned} \tag{B2}$$

This gives a transport equation for f with a collision integral in Fokker-Planck form,

$$\frac{df}{dt} = \mathcal{I}[f], \quad \mathcal{I}[f] = \frac{\partial}{\partial p}\left(A_p f + \frac{\partial}{\partial p}[B_p f] \right). \tag{B3}$$

The transport coefficients are given by

$$A_p = \sum_q q P(p,q), \quad B_p = \frac{1}{2}\sum_q q^2 P(p,q), \tag{B4}$$

where q is the momentum transferred between the heavy object and the light one in a single collision.

For the dark soliton we write the momentum $p = -M v_s$, giving the collision integral as a function of velocity,

$$\mathcal{I}[f] = \frac{\partial}{\partial v_s}\left(-\frac{A_p}{M} f + \frac{\partial}{\partial v_s}\left[\frac{B_p}{M^2} f \right] \right) \tag{B5}$$

$$= \frac{\partial}{\partial v_s}\left(-A_{v_s} f + \frac{\partial}{\partial v_s}[B_{v_s} f] \right). \tag{B6}$$

The transport coefficients presented in Eqs. (13) and (14) of the main text are related to A_p and B_p as $A_{v_s} = A_p/M$ and $B_{v_s} = B_p/M^2$; we present the rest of the calculation in terms of v_s.

Coefficients A_{v_s} and B_{v_s} are not independent. When $f = \exp[-E(v_s)/k_B T]$ is the Maxwell-Boltzmann distribution, the collision integral $\mathcal{I}[f]$ must vanish. For the soliton, we have $f(E(v_s)) \approx \exp(M v_s^2/2k_B T)$. Plugging this into $\mathcal{I}[f]$, we find the relation

$$\left(-A_{v_s} + \frac{\partial B_{v_s}}{\partial v_s} \right) f + \frac{v_s M B_{v_s}}{k_B T} f = 0. \tag{B7}$$

To first order, $\partial_{v_s} B_{v_s} = 0$, giving

$$A_{v_s} = \frac{M v_s B_{v_s}}{k_B T}. \tag{B8}$$

We emphasize that this relation relies only on the condition that $f(E(v_s))$ is Maxwell-Boltzmann and not on the microscopic properties of the scatterers, and the microscopic expressions for A_{v_s} and B_{v_s} must satisfy this relation [40].

The probability per unit time that the heavy object will undergo a scattering event is $P(p,q) = R_q |v_q| \mathbf{s}(k,k_s)$, where R_q is the reflection coefficient, $|v_q|$ is the velocity, and $\mathbf{s}(k,k_s)$ is a statistical factor which gives the occupation number of scatterers. In the case of bosonic impurities, $\mathbf{s}(k,k_s) = n_B(1 + n_B)$, where n_B is the Bose-Einstein distribution. This term accounts for bosonic enhancement.

In the case of fermionic impurities, which we consider here, $\mathbf{s}(k,k_s) = n_F(1 - n_F)$, where n_F is the Fermi-Dirac distribution. This term accounts for Pauli blocking, which means that a fermion with momentum k is unable to scatter into a state with momentum $-k$ if that state is already filled. An incoming particle with momentum $p_i = \hbar k$ is reflected with momentum $p_f = -\hbar k$, giving $q = p_f - p_i = -2\hbar k$. Now, we have the following expressions for A_{v_s} and B_{v_s}:

$$A_{v_s} = -\frac{2\hbar}{M} \sum_k k R_{k,\lambda} \left| \frac{\partial \epsilon_k}{\hbar \partial k} \right| n_F(\epsilon_{k+k_s}) \left[1 - n_F\left(\epsilon_{-k+k_s}\right)\right], \tag{B9}$$

$$B_{v_s} = \frac{2\hbar^2}{M^2} \sum_k k^2 R_{k,\lambda} \left| \frac{\partial \epsilon_k}{\hbar \partial k} \right| n_F(\epsilon_{k+k_s}) \left[1 - n_F\left(\epsilon_{-k+k_s}\right)\right]. \tag{B10}$$

Given these relations, we can check that Eq. (B8) is satisfied to first order in $k_s = m_i v_s/\hbar$. The Fermi-Dirac distribution can be expanded as

$$n_F(\epsilon_{\pm k+k_s}) \approx n_F(\epsilon_{\pm k}) \pm \hbar k v_s \frac{\partial n_F}{\partial \epsilon_{\pm k}}, \tag{B11}$$

where we have used the relation $\epsilon_{\pm k+k_s} \approx \epsilon_{\pm k} \pm \hbar k v_s$. Plugging into Eq. (B9), we find

$$A_{v_s} \approx -\frac{2\hbar^2 v_s}{M} \sum_k k^2 R_{k,\lambda} \left| \frac{\partial \epsilon_k}{\hbar \partial k} \right| \frac{\partial n_F}{\partial \epsilon_k} = \frac{M v_s B_{v_s}}{k_B T}. \tag{B12}$$

We note that the zeroth-order term of A_{v_s} vanishes because $\sum_k k$ is an odd function of k. Similarly, for B_{v_s} the first order in k_s is $B \propto \sum_k k^3 = 0$. Equation (B8) is satisfied *only* if the Pauli-blocking term is included in the microscopic expressions for A_{v_s} and B_{v_s}.

APPENDIX C: SOLUTION OF THE KINETIC EQUATION FOR A SOLITON IN A HARMONIC TRAP

Here we present an analytical solution of Eq. (16) for a soliton in a harmonic trap with potential $U(x) = -M\omega^2 x^2/2$. In the following it is instructive to introduce dimensionless units as follows: $t \to t/\Gamma, \omega \to \omega\Gamma, v_s \to v_{th} v_s, x \to v_{th} x/\Gamma$. The kinetic equation is given by

$$\frac{\partial f}{\partial t} + v_s \frac{\partial f}{\partial x_s} - \omega^2 x_s \frac{\partial f}{\partial v_s} = \frac{\partial}{\partial v_s}\left(-v_s f + \frac{\partial f}{\partial v_s}\right), \tag{C1}$$

where $\Gamma = \gamma/M$ and $v_{th}^2 = k_B T/M$ can be interpreted as the thermal velocity. Equation (C1) needs to be supplemented by the initial conditions. We assume that the soliton is created in the trap center with initial velocity v_i, resulting in $f(0,x_s,v_s) = \delta(x_s)\delta(v_s - v_i)$. This second-order partial differential equation (PDE) can be reduced to first order by Fourier transform. Setting

$$f(t,x_s,v_s) = \sum_{p,q} \bar{f}(t,p,q) e^{ipx_s + iqv_s}, \tag{C2}$$

we find the following first-order PDE:

$$\frac{\partial \bar{f}}{\partial t} - (p+q)\frac{\partial \bar{f}}{\partial q} + \omega^2 q \frac{\partial \bar{f}}{\partial p} = -q^2 \bar{f}, \tag{C3}$$

with the transformed initial condition $\tilde{f}(0,p,q) = e^{-iqv_i}$. Equation (C3) can be solved analytically using the method of characteristics. According to the method, the PDE can be transformed to a system of ordinary differential equations (ODEs) along characteristic lines, parametrized by s and defined as follows:

$$\frac{d\bar{f}'}{ds} = -q^2(s)\bar{f}, \quad \frac{dt}{ds} = 1, \quad \frac{dq}{ds} = -[p(s) + q(s)], \quad \frac{dp}{ds} = \omega^2 q(s), \tag{C4}$$

$$\bar{f}'(0) = \bar{f}(0,p_0,q_0), \quad t(0) = 0, \quad q(0) = q_0, \quad p(0) = p_0, \tag{C5}$$

where we introduced $\bar{f}'(s) = f(t(s),p(s),q(s))$ and Eqs. (C5) are the initial conditions written in a general form. Integration of (C4) results in

$$\bar{f}(s) = \exp(Z), \tag{C6}$$

$$Z = \frac{e^{-s}}{8\omega^2\bar{\omega}^2}\left[4\omega^2 p_0(p_0+q_0) + 4q_0^2\omega^4 - \left(p_0^2 + 4p_0q_0\omega^2 + q_0^2\omega^2\right)\cos(2\bar{\omega}s) + 2\bar{\omega}\left(p_0^2 - q_0^2\omega^2\right)\sin(2\bar{\omega}s)\right] - \frac{q_0\omega^2 + p_0^2}{2\omega^2} - iq_0v_i,$$

$$t(s) = s, \quad p(s) = \frac{e^{-s/2}}{\bar{\omega}}\left[p_0\bar{\omega}\cos(\bar{\omega}s) + \frac{p_0 + 2q_0\omega^2}{2}\sin(\bar{\omega}s)\right], \quad q(s) = \frac{e^{-s/2}}{\bar{\omega}}\left[q_0\bar{\omega}\cos(\bar{\omega}s) - \frac{2p_0 + q_0}{2}\sin(\bar{\omega}s)\right], \tag{C7}$$

where $\bar{\omega} = \sqrt{\omega^2 - 1/4}$. For each initial point q_0, p_0 and the parameter s we have the corresponding point $t(s,q_0,p_0)$, $q(s,q_0,p_0)$, $p(s,q_0,p_0)$ on the characteristic line along with $f'(s)$. After inversion of these relations $s(t,q,p)$, $q_0(t,q,p)$, $p_0(t,q,p)$ the general form of the solution of the kinetic equation in the Fourier space is $\bar{f}(t,q,p) = \bar{f}'(s(t,q,p))$. The

inversion of Eqs. (C7) leads to

$$s = t, \quad p_0 = \frac{e^{t/2}}{\bar{\omega}}\left[p\bar{\omega}\cos(\bar{\omega}t) - \frac{p+2q\omega^2}{2}\sin(\bar{\omega}t)\right],$$
$$q_0 = \frac{e^{t/2}}{\bar{\omega}}\left[q\bar{\omega}\cos(\bar{\omega}t) + \frac{2p+q}{2}\sin(\bar{\omega}t)\right], \tag{C8}$$

where Eqs. (C8) satisfy initial conditions (C5). Finally, the general solution in Fourier space is given by

$$\tilde{f}(t,p,q) = \exp\{-g_1(t,\omega)p^2 + g_2(t,\omega)pq - g_3(t,\omega)q^2 - i v_\mathrm{i}[g_4(t,\omega)p + g_5(t,\omega)q]\}, \tag{C9}$$

parametrized by the functions $g_i(t,\omega)$, where

$$g_1(t,\omega) = \frac{4\bar{\omega}^2(e^t-1) - e^t[\cos(2\bar{\omega}t) + 2\bar{\omega}\sin(2\bar{\omega}t) - 1]}{8\omega^2\bar{\omega}^2}, \tag{C10}$$

$$g_2(t,\omega) = \frac{e^t}{2\bar{\omega}^2}[\cos(2\bar{\omega}t) - 1], \tag{C11}$$

$$g_3(t,\omega) = \frac{4\bar{\omega}^2(e^t-1) + e^t[2\bar{\omega}\sin(2\bar{\omega}t) - \cos(\bar{\omega}t) + 1]}{8\bar{\omega}^2}, \tag{C12}$$

$$g_4(t,\omega) = \frac{e^{t/2}}{\bar{\omega}}\sin(\bar{\omega}t), \tag{C13}$$

$$g_5(t,\omega) = \frac{e^{t/2}}{\bar{\omega}}\left[\bar{\omega}\cos(\bar{\omega}t) + \frac{1}{2}\sin(\bar{\omega}t)\right]. \tag{C14}$$

Equation (C3) does not have a stationary solution where $\partial\tilde{f}/\partial t \to 0$ due to the negative drift term, which causes the distribution to drift to higher velocities. Equation (C9) grows exponentially at long times; this is an artifact of the linear approximation for soliton momentum, $p \approx -Mv$. The approach is equally valid for the full soliton spectrum in Eq. (10), which is bounded, but does not admit an exact analytical solution. Finally, transforming Eq. (C9) back to real space, we find the full distribution function $f(t,x_\mathrm{s},v_\mathrm{s})$ with Gaussian form,

$$f(t,x_\mathrm{s},v_\mathrm{s}) = \frac{1}{2\pi\sqrt{4g_1g_3 - g_2^2}}\exp\left\{-\frac{1}{4g_1g_3 - g_2^2}\left[g_1v_\mathrm{s}^2 + g_3x_\mathrm{s}^2 + g_2v_\mathrm{s}x_\mathrm{s} - v_\mathrm{i}v_\mathrm{s}(g_2g_4 + 2g_1g_5) - v_\mathrm{i}x_\mathrm{s}(g_2g_5 + 2g_3g_4) + v_\mathrm{i}^2\left(g_3g_4^2 + g_1g_5^2 + g_2g_4g_5\right)\right]\right\}. \tag{C15}$$

The distribution contains all information about the stochastic dynamics of a dark soliton. The time dependence of the average soliton position and variance in position are given by

$$\bar{x}_\mathrm{s}(t) = \int_{-\infty}^{\infty}dv_\mathrm{s}\int_{-\infty}^{\infty}dx_\mathrm{s}x_\mathrm{s}f(t,x_\mathrm{s},v_\mathrm{s}) = v_\mathrm{i}g_4(t,\omega) \to \frac{v_\mathrm{i}e^{\Gamma t/2}}{\bar{\omega}}\sin(\bar{\omega}t), \tag{C16}$$

$$D_x(t) = \int_{-\infty}^{\infty}dv_\mathrm{s}\int_{-\infty}^{\infty}dx_\mathrm{s}x_\mathrm{s}^2f(t,x_\mathrm{s},v_\mathrm{s}) = 2g_1(t,\omega) + v_\mathrm{i}^2g_4^2(t,\omega) \to \frac{v_\mathrm{i}^2e^{\Gamma t}}{\bar{\omega}^2}\sin^2(\bar{\omega}t) + \frac{v_\mathrm{th}^2(e^{\Gamma t}-1)}{\bar{\omega}^2} - \frac{v_\mathrm{th}^2\Gamma^2e^{\Gamma t}}{4\omega^2\bar{\omega}^2}\left(\cos(2\bar{\omega}t) + \frac{2\bar{\omega}}{\Gamma}\sin(2\bar{\omega}t) - 1\right), \tag{C17}$$

where $\bar{\omega} = \sqrt{\omega^2 - \Gamma^2/4}$ in real units. Similarly, the average velocity and variance in velocity are given by

$$\bar{v}_\mathrm{s}(t) = \int_{-\infty}^{\infty}dv_\mathrm{s}\int_{-\infty}^{\infty}dx_\mathrm{s}v_\mathrm{s}f(t,x_\mathrm{s},v_\mathrm{s}) = v_\mathrm{i}g_5(t,\omega) \to \frac{v_\mathrm{i}e^{\Gamma t/2}}{\bar{\omega}}\left[\bar{\omega}\cos(\bar{\omega}t) + \frac{\Gamma}{2}\sin(\bar{\omega}t)\right], \tag{C18}$$

$$D_v(t) = \int_{-\infty}^{\infty}dv_\mathrm{s}\int_{-\infty}^{\infty}dx_\mathrm{s}v_\mathrm{s}^2f(t,x_\mathrm{s},v_\mathrm{s}) = 2g_3(t,\omega) + v_\mathrm{i}^2g_5(t,\omega)^2 \to \frac{v_\mathrm{i}^2e^{\Gamma t}}{\bar{\omega}^2}\left[\bar{\omega}\cos(\bar{\omega}t) + \frac{\Gamma}{2}\sin(\bar{\omega}t)\right]^2 + v_\mathrm{th}^2(e^{\Gamma t}-1) + \frac{\Gamma^2v_\mathrm{th}^2e^{\Gamma t}}{4\bar{\omega}^2}\left(\frac{2\bar{\omega}}{\Gamma}\sin(2\bar{\omega}t) - \cos(2\bar{\omega}t) + 1\right). \tag{C19}$$

APPENDIX D: CALCULATION OF SOLITON LIFETIME

The lifetime of a dark soliton depends on its velocity; when the soliton reaches the condensate speed of sound c, its depth is zero, and it disappears. Integrating Eq. (C15) over spatial coordinate x_s, we find the distribution function only in terms of velocity:

$$f_v(t,v_\mathrm{s}) = \frac{1}{\sqrt{4\pi g_3(t,\omega)}}\exp\left(-\frac{[v_\mathrm{s} - \bar{v}_\mathrm{s}(t)]^2}{4g_3(t,\omega)}\right), \tag{D1}$$

where $g_3(t,\omega)$ is given by Eq. (C12) and $\bar{v}_\mathrm{s}(t)$ is Eq. (C18) in Appendix C.

We consider a perfectly absorbing boundary condition at $v_\mathrm{s} = \pm c$ which accounts for the soliton disappearance. The boundary condition imposed is $f_v(\pm c,t) = 0$ for all times t. We construct a distribution that obeys this boundary condition using the method of images. The distribution function is reflected about the boundaries, $v_\mathrm{s} = \pm c$ in our case, with "image distributions" placed at $v_n = 2cn$ for $n = \pm1, \pm2, \ldots$. The distribution which obeys the boundary condition is then

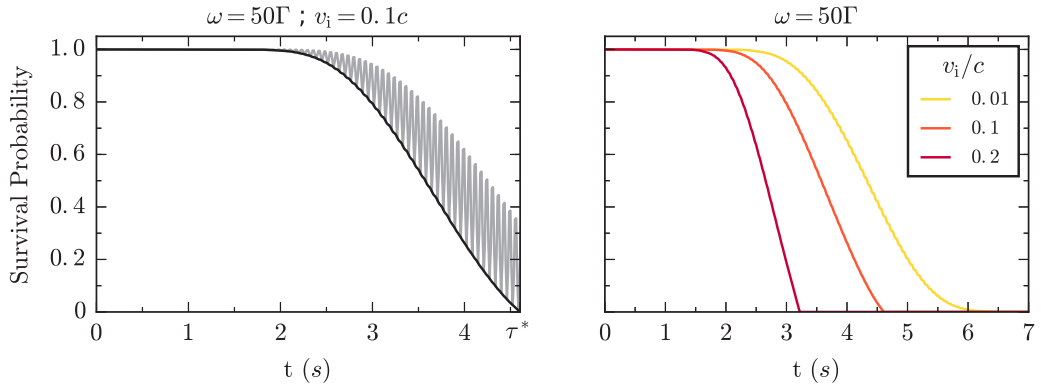

FIG. 6. Left: Survival probability as defined by the exact expression in Eq. (D4) (gray line) is highly oscillatory due to the dynamics in the trap. The lower bound is given by replacing $\bar{v}_s(t)$ with Eq. (D5) (black line). Soliton lifetime is marked by τ_s on the horizontal axis. Calculated for $v_i = 0.1c$ and $\omega = 50\Gamma$. Right: Survival probability for different soliton initial velocities with $\omega = 50\Gamma$. Survival probability falls off more quickly for faster initial velocities, with the fastest initial velocity indicated by the red (dark gray) line.

described by the general formula

$$f_v^{\mathrm{Img}}(t,v_s) = f_v(t,v_s) + \sum_{n=1}^{\infty}(-1)^n[f_v(t,v_n - v) + f_v(t,-v_n - v)], \quad v_n = 2cn. \tag{D2}$$

We find the total survival probability of the soliton by integrating over v_s from $-c$ to c,

$$\mathcal{P}(|v_s| < c;t) = \int_{-c}^{c} dv_s f_{v_s}^{\mathrm{Img}}(v_s,t). \tag{D3}$$

Since each term in $f_{v_s}^{\mathrm{Img}}(v_s,t)$ is a Gaussian, we integrate and find the following expression for the survival probability:

$$\mathcal{P}(|v_s|<c;t) = \frac{1}{2}\left(\mathrm{Erf}\left[\frac{c-\bar{v}_s(t)}{2\sqrt{g_3(t,\omega)}}\right] + \mathrm{Erf}\left[\frac{c+\bar{v}_s(t)}{2\sqrt{g_3(t,\omega)}}\right]\right) + \frac{1}{2}\sum_{n=1}^{\infty}(-1)^n\left(\mathrm{Erf}\left[\frac{c+v_n-\bar{v}_s(t)}{2\sqrt{g_3(t,\omega)}}\right] + \mathrm{Erf}\left[\frac{c-v_n-\bar{v}_s(t)}{2\sqrt{g_3(t,\omega)}}\right] + \mathrm{Erf}\left[\frac{c-v_n+\bar{v}_s(t)}{2\sqrt{g_3(t,\omega)}}\right] + \mathrm{Erf}\left[\frac{c+v_n+\bar{v}_s(t)}{2\sqrt{g_3(t,\omega)}}\right]\right). \tag{D4}$$

The exact expression in Eq. (D4) is oscillatory because $\bar{v}_s(t)$ and $g_3(t,\omega)$ capture oscillations in the trap as well as the long-time acceleration of the soliton. However, if the soliton velocity reaches c at any point in its oscillation, it will not survive, so we focus on the lower bound of $\mathcal{P}(|v_s| < c;t)$, which can be found by replacing $\bar{v}_s(t) \to \bar{v}_s^*(t)$, where $\bar{v}_s^*(t)$ is the maximum value over one oscillation period,

$$\bar{v}_s^*(t) = \frac{v_i e^{\Gamma t/2}}{\bar{\omega}}\sqrt{\bar{\omega}^2 + \Gamma^2/4} = \frac{v_i \omega e^{\Gamma t/2}}{\bar{\omega}}. \tag{D5}$$

Making this substitution, we can plot a smooth survival probability curve. When $|\bar{v}_s^*(\tau_s)| = c$, $\mathcal{P}(|v_s| < c;\tau_s) = 0$, and we define τ_s as the soliton lifetime. The exact oscillatory expression and the lower envelope of the survival probability are shown in Fig. 6.

[1] S. Burger, K. Bongs, S. Dettmer, W. Ertmer, K. Sengstock, A. Sanpera, G. V. Shlyapnikov, and M. Lewenstein, Dark Solitons in Bose-Einstein Condensates, Phys. Rev. Lett. **83**, 5198 (1999).

[2] J. Denschlag, J. E. Simsarian, D. L. Feder, Charles W. Clark, L. A. Collins, J. Cubizolles, L. Deng, E. W. Hagley, K. Helmerson, W. P. Reinhardt, S. L. Rolston, B. I. Schneider, and W. D. Phillips, Generating solitons by phase engineering of a Bose-Einstein condensate, Science **287**, 97 (2000).

[3] L. Khaykovich, F. Schreck, G. Ferrari, T. Bourdel, J. Cubizolles, L. D. Carr, Y. Castin, and C. Salomon, Formation of a matter-wave bright soliton, Science **296**, 1290 (2002).

[4] K. E. Strecker, G. B. Partridge, A. G. Truscott, and R. G. Hulet, Formation and propagation of matter-wave soliton trains, Nature (London) **417**, 150 (2002).

[5] T. Yefsah, A. T. Sommer, M. J. H. Ku, L. W. Cheuk, W. Ji, W. S. Bakr, and M. W. Zwierlein, Heavy solitons in a fermionic superfluid, Nature (London) **499**, 426 (2013).

[6] C. Becker, S. Stellmer, P. Soltan-Panahi, S. Dörscher, M. Baumert, E-M. Richter, J. Kronjäger, K. Bongs, and K. Sengstock, Oscillations and interactions of dark and dark-bright solitons in Bose-Einstein condensates, Nat. Phys. **4**, 496 (2008).

[7] J. Ieda, T. Miyakawa, and M. Wadati, Exact Analysis of Soliton Dynamics in Spinor Bose-Einstein Condensates, Phys. Rev. Lett. **93**, 194102 (2004).

[8] T. Karpiuk, K. Brewczyk, S. Ospelkaus-Schwarzer, K. Bongs, M. Gajda, and K. Rzażewski, Soliton Trains in Bose-Fermi Mixtures, Phys. Rev. Lett. **93**, 100401 (2004).

[9] H. Tercas, D. D. Solnyshkov, and G. Malpuech, Topological Wigner Crystal of Half-Solitons in a Spinor Bose-Einstein Condensate, Phys. Rev. Lett. **110**, 035303 (2013).

[10] H. Tercas, D. D. Solnyshkov, and G. Malpuech, High-Speed DC Transport of Emergent Monopoles in Spinor Photonic Fluids, Phys. Rev. Lett. **113**, 036403 (2014).

[11] C. Qu, L. P. Pitaevskii, and S. Stringari, Magnetic Solitons in a Binary Bose-Einstein Condensate, Phys. Rev. Lett. **116**, 160402 (2016).
[12] Hans-Benjamin Braun and Daniel Loss, Berry's phase and quantum dynamics of ferromagnetic solitons, Phys. Rev. B **53**, 3237 (1996).
[13] C. H. Wong and Y. Tserkovnyak, Dissipative dynamics of magnetic solitons in metals, Phys. Rev. B **81**, 060404 (2010).
[14] S. K. Kim, Y. Tserkovnyak, and O. Tchernyshyov, Propulsion of a domain wall in an antiferromagnet by magnons, Phys. Rev. B **90**, 104406 (2014).
[15] S. K. Kim, O. Tchernyshyov, and Y. Tserkovnyak, Thermophoresis of an antiferromagnetic soliton, Phys. Rev. B **92**, 020402 (2015).
[16] C. Psaroudaki, S. Hoffman, J. Klinovaja, and D. Loss, Quantum dynamics of skyrmions in chiral magnets, arXiv:1612.01885.
[17] J. Anglin, Atomic dark solitons: Quantum canaries learn to fly, Nat. Phys. **4**, 437 (2008).
[18] P. O. Fedichev, A. E. Muryshev, and G. V. Shlyapnikov, Dissipative dynamics of a kink state in a Bose-condensed gas, Phys. Rev. A **60**, 3220 (1999).
[19] D. K. Efimkin and V. Galitski, Moving solitons in a one-dimensional fermionic superfluid, Phys. Rev. A **91**, 023616 (2015).
[20] R. G. McDonald and A. S. Bradley, Brownian motion of a matter-wave bright soliton moving through a thermal cloud of distinct atoms, Phys. Rev. A **93**, 063604 (2016).
[21] D. K. Efimkin, J. Hofmann, and V. Galitski, Non-Markovian Quantum Friction of Bright Solitons in Superfluids, Phys. Rev. Lett. **116**, 225301 (2016).
[22] B. Jackson, N. P. Proukakis, and C. F. Barenghi, Dark-soliton dynamics in Bose-Einstein condensates at finite temperature, Phys. Rev. A **75**, 051601 (2007).
[23] S. P. Cockburn, H. E. Nistazakis, T. P. Horikis, P. G. Kevrekidis, N. P. Proukakis, and D. J. Frantzeskakis, Fluctuating and dissipative dynamics of dark solitons in quasi-condensates, Phys. Rev. A **84**, 043640 (2011).
[24] A. Muryshev, G. V. Shlyapnikov, W. Ertmer, K. Sengstock, and M. Lewenstein, Dynamics of Dark Solitons in Elongated Bose-Einstein Condensates, Phys. Rev. Lett. **89**, 110401 (2002).
[25] S. Sinha, A. Y. Cherny, D. Kovrizhin, and J. Brand, Friction and Diffusion of Matter-Wave Bright Solitons, Phys. Rev. Lett. **96**, 030406 (2006).
[26] L. M. Aycock, H. M. Hurst, D. K. Efimkin, D. Genkina, H.-I. Lu, V. M. Galitski, and I. B. Spielman, Brownian motion of solitons in a Bose-Einstein condensate, Proc. Natl. Acad. Sci. USA **114**, 2503 (2017).
[27] B. A. Ivanov and A. K. Kolezhuk, Soliton diffusion in one-dimensional systems close to integrable ones, Phys. Lett. A **146**, 190 (1990).
[28] N. G. Parker, N. P. Proukakis, M. Leadbeater, and C. S. Adams, Soliton-Sound Interactions in Quasi-One-Dimensional Bose-Einstein Condensates, Phys. Rev. Lett. **90**, 220401 (2003).
[29] N. G. Parker, N. P. Proukakis, and C. S. Adams, Dark soliton decay due to trap anharmonicity in atomic Bose-Einstein condensates, Phys. Rev. A **81**, 033606 (2010).
[30] Th. Busch and J. R. Anglin, Dark-Bright Solitons in Inhomogeneous Bose-Einstein Condensates, Phys. Rev. Lett. **87**, 010401 (2001).
[31] A. Einstein, On the movement of small particles suspended in stationary liquids required by the molecular-kinetic theory of heat, Ann. Phys. (Berlin, Ger.) **17**, 549 (1905).
[32] M. Olshanii, Atomic Scattering in the Presence of an External Confinement and a Gas of Impenetrable Bosons, Phys. Rev. Lett. **81**, 938 (1998).
[33] A. Imambekov and E. Demler, Exactly solvable case of a one-dimensional Bose-Fermi mixture, Phys. Rev. A **73**, 021602 (2006).
[34] C. K. Lai and C. N. Yang, Ground-state energy of a mixture of fermions and bosons in one dimension with a repulsive δ-function interaction, Phys. Rev. A **3**, 393 (1971).
[35] A. G. Truscott, K. E. Strecker, W. I. McAlexander, G. B. Partridge, and R. G. Hulet, Observation of Fermi pressure in a gas of trapped atoms, Science **291**, 2570 (2001).
[36] F. Schreck, L. Khaykovich, K. L. Corwin, G. Ferrari, T. Bourdel, J. Cubizolles, and C. Salomon, Quasipure Bose-Einstein Condensate Immersed in a Fermi Sea, Phys. Rev. Lett. **87**, 080403 (2001).
[37] Z. Hadzibabic, C. A. Stan, K. Dieckmann, S. Gupta, M. W. Zwierlein, A. Görlitz, and W. Ketterle, Two-Species Mixture of Quantum Degenerate Bose and Fermi Gases, Phys. Rev. Lett. **88**, 160401 (2002).
[38] J. Goldwin, S. Inouye, M. L. Olsen, B. Newman, B. D. DePaola, and D. S. Jin, Measurement of the interaction strength in a Bose-Fermi mixture with ^{87}Rb and ^{40}K, Phys. Rev. A **70**, 021601 (2004).
[39] R. Roy, A. Green, R. Bowler, and S. Gupta, Two-Element Mixture of Bose and Fermi Superfluids, Phys. Rev. Lett. **118**, 055301 (2017).
[40] E. M. Lifschitz and L. P. Pitaevskii, *Physical Kinetics*, Course of Theoretical Physics, Vol. 10 (Oxford, 1983).
[41] G. Pöschl and E. Teller, Bemerkungen zur Quantenmechanik des anharmonischen Oszillators, Z. Phys. **83**, 143 (1933).
[42] A. Frank and K. B. Wolf, Lie Algebras for Potential Scattering, Phys. Rev. Lett. **52**, 1737 (1984).
[43] J. Guerrero, A group-theoretical derivation of the S-matrix for the Pöschl-Teller potentials, J. Phys. Conf. Ser. **237**, 012012 (2010).
[44] Y. Alhassid, F. Gürsey, and F. Iachello, Potential Scattering, Transfer Matrix, and Group Theory, Phys. Rev. Lett. **50**, 873 (1983).
[45] D. Çevik, M. Gadella, Ş. Kuru, and J. Negro, Resonances and antibound states for the Pöschl-Teller potential: Ladder operators and SUSY partners, Phys. Lett. A **380**, 1600 (2016).
[46] M. I. Shaukat, E. V. Castro, and H. Terças, Quantum dark soliton (qubits) in Bose Einstein condensates, arXiv:1701.07903.
[47] V. V. Konotop and L. Pitaevskii, Landau Dynamics of a Grey Soliton in a Trapped Condensate, Phys. Rev. Lett. **93**, 240403 (2004).
[48] Th. Busch and J. R. Anglin, Motion of Dark Solitons in Trapped Bose-Einstein Condensates, Phys. Rev. Lett. **84**, 2298 (2000).
[49] A. Weller, J. P. Ronzheimer, C. Gross, J. Esteve, M. K. Oberthaler, D. J. Frantzeskakis, G. Theocharis, and P. G. Kevrekidis, Experimental Observation of Oscillating and Interacting Matter Wave Dark Solitons, Phys. Rev. Lett. **101**, 130401 (2008).
[50] M. Kitagawa, K. Enomoto, K. Kasa, Y. Takahashi, R. Ciuryło, P. Naidon, and P. S. Julienne, Two-color photoassociation

spectroscopy of ytterbium atoms and the precise determinations of s-wave scattering lengths, Phys. Rev. A **77**, 012719 (2008).

[51] T. Fukuhara, S. Sugawa, Y. Takasu, and Y. Takahashi, All-optical formation of quantum degenerate mixtures, Phys. Rev. A **79**, 021601 (2009).

[52] N. D. Lemke, A. D. Ludlow, Z. W. Barber, T. M. Fortier, S. A. Diddams, Y. Jiang, S. R. Jefferts, T. P. Heavner, T. E. Parker, and C. W. Oates, Spin-1/2 Optical Lattice Clock, Phys. Rev. Lett. **103**, 063001 (2009).

[53] M.-S. Kim, J. Lee, J. H. Lee, Y. Shin, and J. Mun, Measurements of optical Feshbach resonances of ^{174}Yb atoms, Phys. Rev. A **94**, 042703 (2016).

[54] H. Risken, *The Fokker-Planck Equation* (Springer, Berlin, 1984).